Inorganic Chemistry

pubs.acs.org/IC

Article

Strong Triel Bonds with Be as Electron Donor

Xin Wang, Zhihao Niu, Qingzhong Li,* and Steve Scheiner*

Cite This: *Inorg. Chem.* 2024, 63, 14656−14664

Read Online

ACCESS | Metrics & More | Article Recommendations | Supporting Information

ABSTRACT: A systematic theoretical study was conducted on the triel bonds (TrBs) within the $TrX_3\cdots Be(CO)_3$ complexes (Tr = B, Al, Ga, In, Tl; X = H, F, Cl, Br, I). The interaction energies of these systems range between 4 and 38 kcal/mol. The TrB weakens as X becomes more electronegative in the B and Al systems, while the opposite pattern of stronger bonds is observed in the In and Tl analogues. The dominant component of the TrB is polarization energy, which arises from charge transfer from $Be(CO)_3$ to TrX_3. The source of the density is a confluence of CO π-bonding orbitals at the Be center that resembles a Be lone pair, and which makes the molecular electrostatic potential above the Be somewhat negative. This π-lump is paired with the highly positive π-hole above the Tr, and a large amount of charge is transferred to the empty p_z orbital of Tr. These factors, when considered in conjunction with large AIM measures, confer on this TrB a certain degree of covalency.

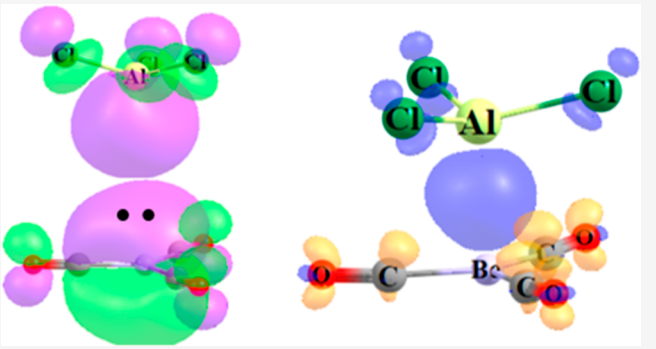

INTRODUCTION

As a fundamental concept in the field of supramolecular chemistry, noncovalent interactions have long been a focus of research, due to their important applications in crystal materials, catalysis, biomolecular functional regulation, molecular recognition, molecular assembly, and other fields.[1−4] The noncovalent interaction formed between the Lewis acid center of a Group 13 atom and an electron donor is termed a triel bond (TrB). Due to its unique molecular structure and wide strength range, the TrB has broad applications in asymmetric catalysis, material construction, dyes, molecular recognition, hydrogen storage, and other fields.[5−7] Due to the electron deficient nature of the Group 13 atomic p_z orbital within the context of planar sp^2 hybridization, there exist positive electrostatic potential regions above the plane, which are referred to as a π-hole.[8] This region is attractive toward nucleophiles and can interact with the electron donor's rich electric region to form a TrB.

As early as the 1960s, TrB complexes had already appeared in people's vision, but the concept of the TrB was not widely disseminated. Grotewold et al. believed that this interaction can serve as a transition state for the S_N2 reaction between $BH_3\cdots CO$ complex and $N(CH_2CH_3)$.[9] When studying the mixture of ethylene/propylene and BF_3 using infrared spectroscopy, the existence of 1:1 van der Waals complexes was confirmed, in which electron deficient BF_3 attached itself to the C═C double bond.[10] Subsequent studies found similar interactions between BF_3 and other electron donors (NH_3, HCN, PhCN, and $N(CH_3)_3$).[11−13] The Fourier transform microwave spectroscopy study of the $CH_3CN\cdots BF_3$ complex found that the N···B bond length is 2.011 Å,[14] which lies between the sum of their covalent radii[15] and the sum of their van der Waals radii.[16] Spectral and theoretical studies on X−$CH_3CN\cdots BF_3$ (X = F, Cl, Br, and I) found that the coordination bonds in the gas phase are very weak, and the N···B distance in the solid phase is very short, indicating the existence of an interaction between N and B.

In the theoretical study of the complex formed by BF_3/AlF_3 and electron donors, Grabowski found that the N atom in HCN and N_2 interacts with B/Al in the direction perpendicular to the BF_3/AlF_3 plane to form a complex with C_{3V} symmetry.[8] In subsequent research, he defined this interaction as a TrB.[8] Usually, this kind of interaction is very strong, and its stability largely depends on the amount of charge transfer. The properties of the electron donor center, the electron withdrawing ability of the substituent, and the feedback bonding effects are also closely related to the strength of the interaction. Investigators have also studied the case of other elements in the 13th group as Lewis acid centers. When different Tr atoms act as Lewis acid centers, the system exhibits different properties and strengths. For example, in theoretical research on the formation of a TrB involving pyrazine, it was found that a stable TrB can be formed between N and Tr (Tr = B, Al and Ga), but the effect of halogen substituents on the strength of the TrB varies with the Tr

Received: May 26, 2024
Revised: July 11, 2024
Accepted: July 16, 2024
Published: July 22, 2024

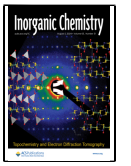

https://doi.org/10.1021/acs.inorgchem.4c02186
Inorg. Chem. 2024, 63, 14656−14664

atom.[17] The order of change in the interaction energy of the system where Al and Ga are located is consistent with the electron withdrawing ability of halogen substituents on Tr atoms, which is F > Cl > Br, while B is exactly the opposite, which is Br > Cl > F.[17]

Theoretical[18] and experimental[19] results confirm that the acidity of BX_3 (X = F, Cl, Br, and I) is $BF_3 < BCl_3 < BBr_3 < BI_3$ when interacting with electron donors. This order is surprising, because it is opposite to the electronegativity pattern of halogen substituents. This phenomenon has been attributed to the back-bond effect.[20] The uniqueness of boron trihalide acidity can also be explained by the charge capacity or ligand closed shell model[21] which can be estimated from ionization potential[22] and electron affinity,[23] respectively. However, these explanations are also controversial, with some studies suggesting that the stronger interaction between BCl_3 and electron donors is due to the fact that BCl_3 has a lower LUMO orbital energy.[24] In weaker interacting systems, the above acidity rule does not hold, but rather F > Cl > Br > H. Experimental results have shown that there are two types of N···B distances in the complexes formed by some boron trihalides with HCN and CH_3CN.[25−28] For the $BF_3\cdots CH_3CN$ complex, two configurations were discovered, with N···B distances of 1.81 and 2.3 Å, respectively, and corresponding binding energies of −7.7 and −8.7 kcal/mol.[26,27] The N···B distances in the two configurations of $BCl_3\cdots CH_3CN$ are 1.60 and 2.69 Å, respectively, corresponding to binding energies of −12.0 and −4.9 kcal/mol.[28] At a shorter N···B distance, CH_3CN acts as a strong electron donor, and the acidity of BCl_3 is stronger than that of BF_3; at a longer N···B, CH_3CN acts as a weak electron donor, and the acidity of BCl_3 is weaker than that of BF_3.

The TrB strength of Group 13 atoms does not have a clear order, as the interaction intensity is not only related to the Tr atom, but also to the type of electron donor and the properties of the substituents. The TrB strength changes in the Al > Ga > In > Tl > B order, but in the $TrF_3\cdots N_2$ system, the positions of Ga and In undergo a reversal.[8] Study of $TrX_3\cdots N$ (Tr = B and Al, X = H and Cl, N = NCH, N_2, NH_3 and Cl^-) showed that in a weak TrB system, the strength of $AlX_3\cdots N_2$ is stronger than that of $BX_3\cdots N_2$, while in a strong TrB system, the order of strength is reversed; but there is an exception in that $AlCl_3\cdots$ NCH is stronger than $BCl_3\cdots$NCH.[29] It appears certain that the orbital interaction where B serves as Lewis acid is the strongest when interacting with a strong electron donor. When forming a strong TrB, the planar triangular molecule BX_3 undergoes significant nonplanar deformation, accompanied by a large deformation energy.[30,31] Significant charge transfer between monomers is crucial in the formation of a TrB, consistent with the strength of Br TrBs. A strong orbital effect often accompanies the high covalency of the TrB. AIM analysis shows that in a strong TrB, the values of the density Laplacian and energy density at the critical bond point corresponding to the TrB are usually positive and negative, respectively, indicating that the TrB in this system has partial covalent properties; when the orbital effect is further enhanced, both become negative.[18,29,30] The Laplacian and energy density at the critical point of weak TrB bonds are usually positive, indicating that such a TrB is a closed shell attraction.[8]

There are many types of electron donors that might participate in a TrB, neutral lone pair electron systems being the most common. Unlike transition metals, there are basically no lone electron pairs in the main group metal atoms, so the main group metal is not typically suitable as a TrB electron donor. However, in some special circumstances, this disadvantage can be eliminated. By shining a strong beam of Nd: YAG laser (532 nm, 60 mj) onto the coating of $NaBH_4$, $(NaBH_3)^-$ can be generated, in which a $Na:\cdots BH_3$ TrB is present. Theoretical calculations indicate that the dissociation energy of this complex is 17.8 kcal/mol, and $Na:^-\cdots B$ is a pure 2c−2e σ bond, as the density arises from a Na 2s lone electron pair. The strength of this $Na:^-\cdots B$ TrB is comparable to that of strong hydrogen bonds and is a partially covalent interaction.[31]

Due to the two outermost 2s electrons, Be typically appears as divalent, and the Be center usually exhibits Lewis acid behavior.[32] On the other hand, the presence of the empty 2p orbital of Be makes it possible to coordinate with molecules containing lone electron pairs. In theoretical research of $Be(CX)_3$(X = O, S, Se, Te and Po), $Be(NH_3)_3$ and $Be(PH_3)_3$, Ariyarathna and Miliordos found that with three σ bond donating substituents, the lone electron pairs of the Be 2s orbital can transfer to the $2p_z$ orbital, and the remaining 2s, $2p_x$, and $2p_y$ orbitals are hybridized to accept the lone electron pairs of three ligands.[33] The calculated dipole moment of the molecule is in good agreement with experiment.[34] The dipole moment of $Be(NH_3)_3$ is 2.5 times that of $Be(PH_3)_3$, indicating that the $Be(NH_3)_3$ molecule has undergone greater polarization.[33] NBO results indicate that in addition to the three interactions between the ligand molecule and the Be σ bond, there is still a π feedback bond from p_z (Be) to the ligand molecule in $Be(CX)_3$ and $Be(PH_3)_3$, while there is no backbond in $Be(NH_3)_3$, which is also the reason for its higher polarization.[33] A similar interaction also exists between Ge and $Be(CX)_3$.[35] A study on $BH_3\cdots BeR_3$ (R = CO, *N*-heterocyclic carbene, and $P(CH_3)_3$) reported a B···Be interaction, and the B···Be bond distance is between 1.989 and 2.196 Å. There is a high degree of delocalization between the electrons on the p_z orbitals of the Be atom and the π electron orbitals of the ligand.[36]

Although the B···Be interaction in which $Be(CX)_3$ participates has been observed in earlier theoretical studies, there has been no systematic study on the nature, strength, and factors influencing the properties of this interaction. In what sort of environment must the electron-deficient Be atom find itself in order to act as an electron donor within a triel bond? What might the mechanism be for this transfer given the absence of a lone pair on Be? Another intriguing aspect is related to whether a Coulombic attraction serves as an important component in the triel bonding of Be, as is typically the case in similar bonds. So the issue arises as to whether the electrostatic potential near the Be atom can be negative, and under what circumstances? With regard to the triel-containing molecule, the obvious question is related to how the TrB might be affected by the identity of this Tr atom, as well as its surrounding ligands. Is there a simple relationship, for example, between Tr size and bond strength, and does the bond weaken or strengthen uniformly as the substituents become more electron-withdrawing?

The Be-containing molecule chosen for quantum chemical study here is $Be(CO)_3$ based in part on past work and because the π-bonding orbitals of CO bear interesting influences on the properties of this molecule. As shown in detail below, these orbitals form the basis for the charge transfer essential to the TrB, and the occurrence of a negative potential on the Be center. The partner Lewis acids comprise the entire TrX_3 series, with Tr = B, Al, Ga, In, and Tl and substituent X runs

https://doi.org/10.1021/acs.inorgchem.4c02186
Inorg. Chem. 2024, 63, 14656−14664

from H to F, Cl, Br, and I. Examination of this full set of 15 different Lewis acids allows a comprehensive understanding of the bonding with $Be(CO)_3$ and the influence of various factors.

THEORETICAL METHODS

All calculations were performed using the Gaussian suite of programs[37] at the B3LYP-D3(BJ)/aug-cc-pVTZ(PP)[38−40] level of theory, using the basis set aug-cc-pVTZ-PP for In, Tl, I, and aug-cc-pVTZ for the smaller atoms. All structures were fully optimized as minima, confirmed by the absence of imaginary frequencies. The interaction energy and binding energy were calculated using the supermolecular method, and the basis set superposition error (BSSE) correction was performed using the counterpoise method proposed by Boys and Bernardi.[41] The interaction energy takes as its reference the energies of the monomers in their geometry within each dyad, while fully optimized monomers are the reference for the binding energy. The Multiwfn program[42] was used to perform topological analysis of the bond critical point (BCP) electron density of the complexes using atoms in molecules (AIM) theory.[43] The interaction region indicator function (IRI) method[44] was used to visualize the TrBs in the complexes. The orbital interactions in the complexes were analyzed using the natural orbitals for chemical valence and the extended transition state method (ETS-NOCV).[45] IRI and ETS-NOCV analyses also utilized the Multiwfn program.[42] The molecular electrostatic potential (MEP) of the monomers on the 0.001 au electron density isosurface were elucidated using the Multiwfn program.[42] Energy decomposition calculations were performed using XEDA[46] software combined with GKS-EDA[47] theory, and XEDA input files were generated using the Mokit program.[48]

RESULTS

Monomers. The molecular electrostatic potential (MEP) surrounding each of the TrX_3 units is similar to that of BCl_3 on the upper part of Figure 1, the principal feature of which is a

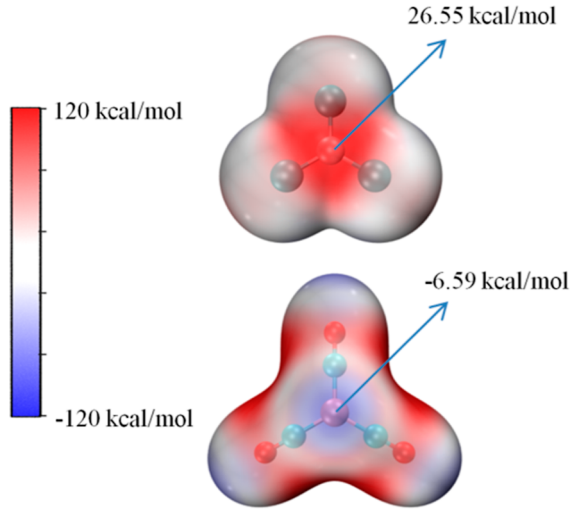

Figure 1. Molecular electrostatic potential (MEP) maps on the 0.001 au electron density isosurface of BCl_3 (upper) and $Be(CO)_3$ (lower). Red and blue regions represent positive and negative MEPs, respectively.

red positive region directly above the central Tr atom as what is commonly termed a π-hole. The MEP of that point is 26.55 kcal/mol, which may be compared with $V_{s,max}$ for the other TrX_3 units in Table 1. For any Tr atom, the π-hole is most prominent for X = F, diminishing along with the electronegativity of the X atom: F > Cl > Br > I. $V_{s,max}$ for X = H lies somewhere in this range, with its relative magnitude dependent

Table 1. Maximum MEP ($V_{s,max}$, kcal/mol) on the 0.001 au Electron Density Isosurface Directly above the Tr Atom of TrX_3

	B	Al	Ga	In	Tl
H	41.35	73.06	59.18	57.18	47.31
F	53.35	112.04	89.70	92.01	75.56
Cl	26.55	70.01	60.33	70.13	60.35
Br	20.94	59.31	51.28	61.11	53.67
I	18.83	47.18	40.07	49.80	45.04

on Tr. The MEP maximum is the smallest for Tr = B, but is somewhat erratic for the other Tr atoms. When X = F, for example, $V_{s,max}$ diminishes in the order Al > In > Ga > Tl > B, but In takes the lead for X = I: In > Al > Tl > Ga > B. In broader terms, the π-hole is sufficiently deep that it ought to sustain a stabilizing interaction with a negative region on the MEP of a partner molecule.

Although the Be atom of $Be(CO)_3$ does not contain a lone electron pair, its surrounding MEP nonetheless contains a negative region, a "π-lump", directly above its central Be. The minimum in this MEP is equal to −6.59 kcal/mol, large enough in magnitude that it should be attracted to the positive π-hole of any of the TrX_3 units. This accumulation of negative potential is present despite an overall positive natural charge of +1.14 on the Be center. As described in greater detail below, the buildup of density above the Be is largely the result of a confluence of C−O π-bonding orbitals of its three ligands.

Geometries and Energetics. The complexes formed when each of the TrX_3 units is paired with $Be(CO)_3$ is exhibited in Figure 2 for $AlCl_3$ which is emblematic of the

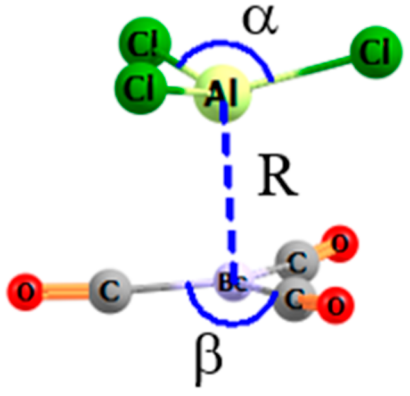

Figure 2. Optimized structure of $AlCl_3\cdots Be(CO)_3$ defining geometrical parameters.

entire set. The two molecules approach one another in a parallel stacked fashion with C_{3v} symmetry, and the TrX_3 becomes somewhat pyramidal. Its degree of nonplanarity can be measured by the sum of the three equal α angles, and its deviation from 360°, while any nonplanarity introduced into the $Be(CO)_3$ is measured by the sum of β angles. As described in greater detail below, the latter remains very nearly planar while the former becomes pyramidal. In most cases, the planarity of TrX_3 diminishes as the X atom grows larger, with a particularly large step between H and F. This same progression from H to I also leads to a steady contraction of the intermolecular separation R, listed in the first column of Table 2. With regard to the Tr series, R is shortest for B then grows longer in an irregular pattern of Ga < Al < In ∼ Tl. One prime

https://doi.org/10.1021/acs.inorgchem.4c02186
Inorg. Chem. 2024, 63, 14656−14664

Table 2. Tr···Be Distance (R, Å), Interaction Energy (E_{int}, kcal/mol), Binding Energy (E_b, kcal/mol), and Deformation Energy (DE, kcal/mol) in TrX_3···$Be(CO)_3$ Complexes

	R	E_{int}	E_b	DE
BH_3	2.264	−20.26	−14.64	5.62
BF_3	3.169	−3.96	−3.35	0.61
BCl_3	2.195	−26.60	−4.05	22.55
BBr_3	2.044	−36.58	−9.53	27.05
BI_3	1.970	−42.25	−16.15	26.10
AlH_3	2.689	−16.61	−14.16	2.45
AlF_3	2.562	−27.73	−20.20	7.53
$AlCl_3$	2.541	−29.81	−20.67	9.14
$AlBr_3$	2.536	−30.53	−21.52	9.01
AlI_3	2.512	−30.54	−22.27	8.27
GaH_3	2.679	−16.31	−14.00	2.31
GaF_3	2.462	−36.66	−25.99	10.67
$GaCl_3$	2.464	−34.56	−23.24	11.32
$GaBr_3$	2.526	−29.72	−22.15	7.57
GaI_3	2.460	−31.87	−22.56	9.31
InH_3	2.845	−15.33	−13.58	1.75
InF_3	2.590	−38.13	−30.03	8.10
$InCl_3$	2.615	−33.91	−26.08	7.83
$InBr_3$	2.626	−32.22	−25.12	7.10
InI_3	2.643	−29.59	−23.61	5.98
TlH_3	2.917	−13.52	−12.35	1.17
$TlCl_3$	2.593	−36.48	−27.50	8.98
$TlBr_3$	2.619	−33.15	−25.57	7.58
TlI_3	2.659	−28.78	−22.91	5.87

exception is BF_3 which has the longest separation of all at 3.169 Å. It is worth noting that TlF_3 serves as another exception in that this molecule does not engage in a triel-bonded complex with $Be(CO)_3$.

The next three columns of Table 2 report the energetics of these complexes. The interaction energy E_{int} compares the complex with the sum of the monomers, both in the geometry they adopt within the dyad, while binding energy E_b takes the optimized monomer geometries as its reference. As such, these two quantities differ by the deformation energy DE which is needed to distort each monomer to its internal structure within the dimer.

The interaction energies are rather large, some in the neighborhood of 40 kcal/mol, so can be categorized as strong noncovalent bonds. These measures are brought down a bit when the deformation energy is added, with $-E_b$ all less than 30 kcal/mol. Particularly large are the deformation energies of the BX_3 units, some of which are nearly 30 kcal/mol. As one might expect in most triel-bonded complexes,[49] DE bears a strong relationship with the nonplanarity introduced into the TrX_3 unit within the confines of the dyad, as exhibited in Figure 3a. As a result, the binding energies of BX_3 are generally rather small, 15 kcal/mol or less. The dependence of the interaction energy on X is rather irregular. While this quantity drops in the order F > Cl > Br > I for most of the Tr atoms, this order reverses for Al and B where it is the heavier X atoms that have the largest E_{int}. It might be noted finally that the energetic patterns in Table 2 are quite distinct from the more regular variation of $V_{s,max}$ in Table 1. One might regard this distinction as a clue that the binding is not dominated by electrostatic energy.

The details of the geometric changes that occur upon complexation within both the Lewis acid and base molecules

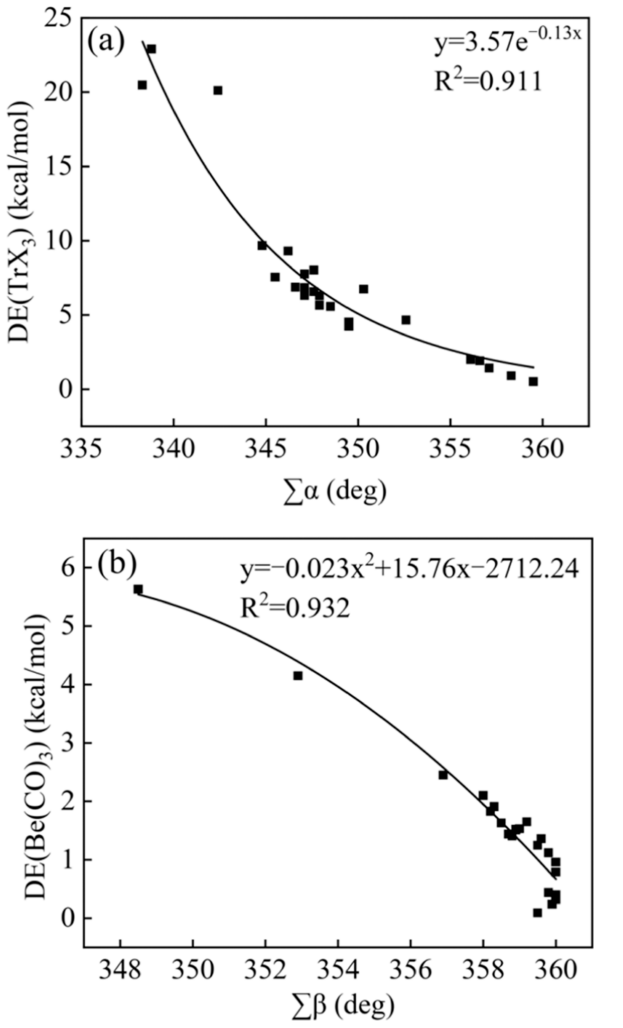

Figure 3. Relationship between (a) the sum of the three X−B−X angles ($\sum\alpha$) and deformation energy of TrX_3 ($DE(TrX_3)$) and (b) the sum of three C−Be−C angles ($\sum\beta$) and deformation energy of $Be(CO)_3$ ($DE(Be(CO)_3)$).

are documented in Table S3. There are elongations of the Tr-X bonds as well as Be−C, while the C≡O bonds suffer a small contraction. Whereas the TrX_3 molecules become rather pyramidal, there is little loss of planarity within the $Be(CO)_3$ unit where the sum of the three β angles varies very little from 360°. As a result, most of the total deformation energy is associated with the Lewis acid unit, as may be seen by a comparison between the last two columns of Table S3. The manner in which the deformation energy of each unit scales with the degree of pyramidal character is explicitly depicted in Figure 3.

Analysis of Electronic Structure. AIM analysis of the electron density topology shows a bond path between the Be and Tr atoms. The principal features of the bond critical point are displayed in Table S1 which are generally commensurate with interaction energies in Table 2. The density lies in the general range between 0.02 and 0.04 au, with some larger values for Tr = B. As is commonly the case, ρ is closely related to the intermolecular separation, as is plainly shown in Figure 4. Both the density Laplacian and total energy density H are negative, suggestive of a certain degree of covalency within the triel bonds, again consistent with the large interaction energies. Cremer and Kraka[50] had suggested as an important quantity

https://doi.org/10.1021/acs.inorgchem.4c02186
Inorg. Chem. 2024, 63, 14656−14664

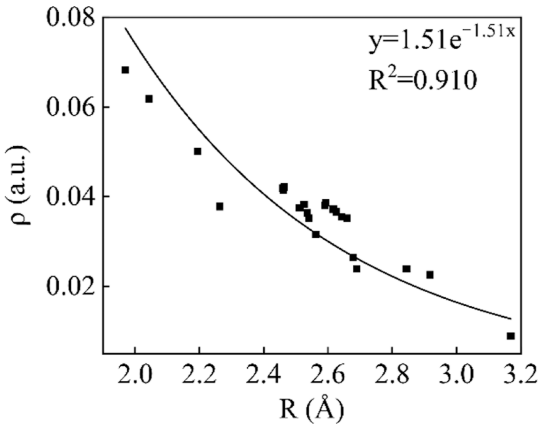

Figure 4. Exponential relationship between the Tr···Be distance (R, Å) and the electron density (ρ, au) at the Tr···Be BCP.

the ratio between potential and kinetic energy density V/G. From the last column of Table S1, it is evident that the absolute values of V/G are all greater than 1, which supports the conclusion of some covalent character. The best correlation with the interaction energy arises with ρ, with a correlation coefficient R^2 of 0.69.

IRI analyses can add further insights into the nature of the bonding in these complexes. Figure S1 contains the IRI plots, where red denotes repulsion, blue indicates strong attractive interactions, and green denotes weaker attraction. The BF_3···$Be(CO)_3$ system has a green surface between the monomers, which indicates a weak TrB in the system. For the AlH_3, GaH_3, InH_3, and TlH_3 systems, the contours of the TrB are greenish-blue, which suggests that the strength of their TrBs is similar to that of hydrogen bonds of average strength. The equivalent surfaces of the TrB for the other systems are dark blue, indicating a very strong TrB. These blue surfaces are sandwiched by red contours, which corresponds to repulsive interactions and is associated with shorter interaction distances.

Another point worth noting is that in most systems there are also isosurfaces of different color depths between the three CO ligands and the Tr-X bond, which suggests that the TrB in the system is more than a simple Tr···Be interaction, and that the three CO ligands play a role in stabilizing the complex, a point which is further elaborated below. As the mass of the X atom increases, these secondary interactions vary from absent to present and from weak to strong. The presence of these secondary interactions is also related to the size of Tr. As the mass of the Tr atom decreases, the possibility of the existence of these secondary interactions becomes greater and their strength also increases.

As another window into the fundamental aspects of these TrBs, the total interaction energy was decomposed into its primary contributing factors. The electrostatic (E^{ele}), exchange (E^{ex}), repulsive (E^{rep}), polarization (E^{pol}), dispersive (E^{disp}) and electron correlation (E^{corr}) energies are listed in Table 3. The large values of repulsive energies, some exceeding 300 kcal/mol, are related to the short Tr···Be distance. The exchange energy is the most negative of the four attractive energies, but this term combines with the larger repulsion energy such that their sum is a repulsive positive quantity. Turning to the remaining purely attractive components, it is the polarization energy that is most negative, in some cases rising up well above 100 kcal/mol. Second is E^{ele}, with dispersion/correlation a distant third. The only exception is BF_3···$Be(CO)_3$ which differs from the other complexes in other ways as well.

Table 3. Exchange (E^{ex}), Repulsion (E^{rep}), Electrostatic (E^{ele}), Polarization (E^{pol}), Sum of Dispersion Energies and Electron Correlation Energies ($E^{disp/corr}$) in the Complexes with $Be(CO)_3$, all in kcal/mol

	E^{ex}	E^{rep}	E^{ele}	E^{pol}	$E^{disp/corr}$
BH_3	−74.78	137.19	−26.72	−42.97	−12.86
BF_3	−13.75	25.28	−7.55	−3.43	−4.46
BCl_3	−110.19	215.27	−47.82	−75.58	−8.09
BBr_3	−144.97	287.62	−62.99	−110.63	−5.40
BI_3	−172.99	342.05	−69.86	−135.51	−5.71
AlH_3	−45.87	85.92	−22.24	−27.42	−6.90
AlF_3	−40.77	80.72	−27.39	−37.21	−2.96
$AlCl_3$	−64.60	125.61	−34.50	−50.28	−5.89
$AlBr_3$	−74.06	143.42	−37.76	−55.52	−6.46
AlI_3	−86.27	165.75	−40.56	−61.40	−7.88
GaH_3	−51.11	97.97	−27.68	−26.90	−8.49
GaF_3	−56.78	116.36	−41.39	−53.74	−0.97
$GaCl_3$	−79.25	159.77	−47.50	−62.90	−4.52
$GaBr_3$	−82.14	162.82	−46.13	−57.09	−7.02
GaI_3	−98.28	195.02	−52.22	−69.34	−7.11
InH_3	−45.19	83.38	−19.98	−25.76	−7.68
InF_3	−53.52	103.36	−29.95	−58.19	0.30
$InCl_3$	−68.47	132.4	−33.52	−60.77	−3.40
$InBr_3$	−74.24	143.00	−35.05	−61.36	−4.42
InI_3	−81.35	155.48	−36.08	−61.09	−6.39
TlH_3	−43.51	80.42	−18.91	−23.18	−8.26
$TlCl_3$	−77.67	152.96	−37.13	−73.59	−0.89
$TlBr_3$	−80.58	157.88	−37.42	−70.15	−2.74
TlI_3	−83.50	161.80	−36.77	−64.45	−5.71

Electron Density Shifts. Within the framework of a triel bond, the primary receptor of electron density would typically be the vacant p_z orbital of the TrX_3 unit which adopts a planar structure as a monomer. As this molecule becomes pyramidal within the complex, the LUMO takes on the shape as illustrated in Figure 5a for $AlCl_3$ in its dyad with $Be(CO)_3$, which has the topology of a Al lone pair orbital, albeit an empty one. The Be atom of the partner has no lone pair per se, as its three valence electrons are occupied in the three Be−C σ-bonds. However, the HOMO of $Be(CO)_3$ is interesting in that the three C−O π-bonding orbitals coalesce in such a manner as to yield the orbital displayed in Figure 5a, centered directly over the Be. The overlap between this occupied HOMO and the LUMO of $AlCl_3$ is obvious in Figure 5a, and represents the heart of the bonding between the two subunits.

Besides the spatial overlap between these two orbitals, another factor in the charge transfer is their energy difference. A lower LUMO energy would come closer to the low-lying HOMO energy of the $Be(CO)_3$, so ought to tend to a stronger bonding interaction. The first column of Table 4 reports the energy of the TrX_3 LUMO which tends toward a more negative value for the larger Tr atoms, corresponding roughly to the interaction energies. However, any correlation is imperfect with R^2 only equal to 0.40. The pyramidalization of the TrX_3 has the benefit of shifting more density toward the approaching Be atom, as opposed to the equal distributions on both sides within the planar molecule. An added dividend is that the deviation from planarity also lowers the LUMO energy, bringing it into closer proximity to the $Be(CO)_3$ HOMO. Taking $AlCl_3$ as an example, its LUMO energy is

https://doi.org/10.1021/acs.inorgchem.4c02186
Inorg. Chem. 2024, 63, 14656−14664

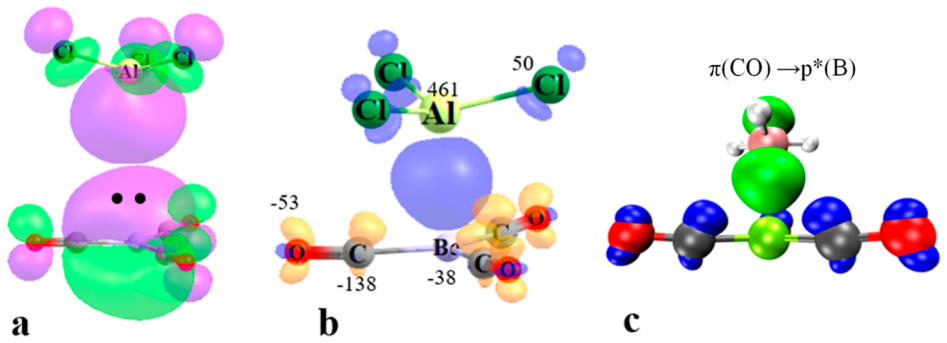

Figure 5. (a) HOMO of $Be(CO)_3$ superposed with the LUMO of $AlCl_3$, where purple and green indicate opposite sign of wave functions. Two dots indicate the two electrons in the occupied HOMO. (b) Electron density shifts occurring as a result of complexation, blue and orange colors signifying gain and loss; ± 0.004 au. Black numbers show change of total density on each atom as assessed by natural atomic occupations, in me. (c) NOCV pair density map of the $\pi(CO) \rightarrow p^*(B)$ in $BH_3\cdots Be(CO)_3$. Green and blue colors indicate gain and loss of density, respectively.

Table 4. Energy of LUMO (ε_{LUMO}, au) and LP*(Tr) (au) of TrX_3 Monomer, Charge Transferred (CT, e) to TrX_3 from $Be(CO)_3$ within Complex, NOCV Orbital Energies (E_{NOCV}, kcal/mol) of the Complexes, and the Difference of Tr−X Bond Length ($\Delta r_{(Tr-X)}$, Å) between the Complex and the Monomer

	ε_{LUMO}	LP*(Tr)	CT	E_{NOCV}	$\Delta r_{(Tr-X)}$
BH_3	−0.083	0.553	0.660	−37.45	0.009
BF_3	−0.019	−0.053	0.049	−3.04	0.004
BCl_3	−0.073		0.893	−53.30	0.081
BBr_3	−0.086		1.089	−74.20	0.110
BI_3	−0.098		1.160	−89.71	0.120
AlH_3	−0.074	−0.041	0.448	−20.14	0.011
AlF_3	−0.078	0.024	0.482	−24.50	0.028
$AlCl_3$	−0.068	−0.054	0.612	−32.85	0.050
$AlBr_3$	−0.074	−0.075	0.642	−36.13	0.057
AlI_3	−0.084	−0.096	0.658	−39.95	0.061
GaH_3	−0.079	−0.056	0.469	−21.18	0.009
GaF_3	−0.111	−0.015	0.663	−35.73	0.044
$GaCl_3$	−0.095	−0.074	0.754	−42.09	0.065
$GaBr_3$	−0.101	−0.089	0.697	−38.76	0.019
GaI_3	−0.113	0	0.755	−46.11	0.073
InH_3	−0.082	−0.065	0.449	−20.08	0.007
InF_3	−0.149	−0.031	0.709	−38.91	0.045
$InCl_3$	−0.129	−0.076	0.756	−41.24	0.059
$InBr_3$	−0.128	−0.085	0.748	−41.55	0.060
InI_3	−0.128	−0.096	0.713	−41.30	0.058
TlH_3	−0.080	−0.066	0.406	−18.70	0.003
$TlCl_3$	−0.165	−0.062	0.830	−48.93	0.076
$TlBr_3$	−0.162	−0.072	0.795	−46.98	0.072
TlI_3	−0.157	−0.086	0.730	−43.66	0.064

lowered by 0.07 au when its planar geometry is deformed into the pyramid within the dyad. The second column of Table 4 contains the energy of the NBO orbital that corresponds to the unoccupied Tr p_z orbital of the monomer. This energy is not a good indicator of the interaction energy, with a correlation coefficient R^2 of only 0.03. Nor does this orbital energy correlate with the total charge transfer CT or polarization energy in Table 3. One quantity which does correlate nicely with CT is the stretch of the internal Tr−X bond in the Lewis acid, with a correlation coefficient of 0.83.

The HOMO−LUMO overlap and resulting charge transfer is a major contributor to overall density displacements as the two subunits are placed near one another, along with polarization effects. Such shifts are visualized in Figure 5b by subtracting the sum of the densities of the two subunits from that of the full complex. The large blue region between the Be and Al atoms corresponds to a density buildup in this bonding area. One can also see smaller orange density depletions on the CO groups whose π-bonding regions participate in the formation of the HOMO which is transferring charge to the $AlCl_3$, with a small amount going to the peripheral Cl centers.

To better quantify these shifts, the black numbers in Figure 5b indicate the change in natural occupation of each atom, in units of me. The large buildup on the Al atom of 461 me is complemented by 50 me increases on each Cl atom. Within the $Be(CO)_3$ unit, it is the set of three C atoms that lose the largest density, each by 138 me. The smallness of the Be density loss is consistent with the formulation of the HOMO as the coalescence of three CO π-bonding orbitals. The third column of Table 4 contains the total charge transferred from $Be(CO)_3$ to TrX_3, as the sum of natural atomic charges on the individual subunits. These transfers are quite large, some even exceeding 1*e*, leading to the idea that these bonds can be thought of as at least partially a dative covalent bond. There is a fairly strong relationship between CT and E_{int}, with a correlation coefficient of 0.72. But more strikingly, CT correlates quite strongly with the polarization energy, with R^2 = 0.93.

Still another picture of the orbital interactions emerges from a NOCV perspective. As another means of studying noncovalent interactions, the ETS-NOCV method can accurately calculate the energy of each orbital through detailed analysis of the density difference between fragments, and it is also very useful to understand the interaction mechanism. The NOCV orbital energies corresponding to the $\pi(CO) \rightarrow p^*(Tr)$ orbital shifts are listed in the penultimate column of Table 4. An example of the NOCV pair density map is provided in Figure 5c for $BH_3\cdots Be(CO)_3$, where density gain and loss are shown respectively by green and blue colors. The similarity of these NOCV changes to those in Figure 5b of full density shifts is evident despite the different TrX_3 units. For the B systems, the NOCV energy order is consistent with the BX_3 acidity as F > H > Cl > Br > I. H and F switch places for Tr = Al. For the Ga system, the positions of Cl and Br are reversed compared to the Al system, and for the In systems, the order of I and Br is reversed compared to Al; for the Tl systems, the order of NOCV energy is consistent with the electronegativity of X, which is H > I > Br > Cl. These NOCV energies are particularly closely correlated with the polarization energy, as is

https://doi.org/10.1021/acs.inorgchem.4c02186
Inorg. Chem. 2024, 63, 14656−14664

clear from perusal of Figure 6. On the other hand, very poor correlation, with R^2 = 0.03, is noted between the interaction energies and the local electron affinity maxima, listed in Table S4.

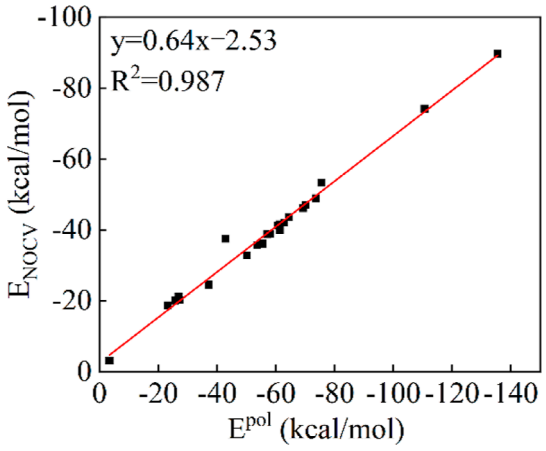

Figure 6. Linear relationship between the polarization energy (E^{pol}) and NOCV orbital energy (E_{NOCV}) in $TrX_3\cdots Be(CO)_3$, all in kcal/mol.

It is of some interest to consider how the various elements that contribute to the binding vary over a range of intermolecular separation. Figure S2a shows how the interaction quickly becomes repulsive as the two subunits in the $BF_3\cdots Be(CO)_3$ complex are moved closer together. At the same time, this closer approach would be favored by a growing charge transfer and NOCV energy, as seen in Figure S2b,c. The individual components of the energy decomposition are illustrated in Figure S3, and shows that the electrostatic, exchange, polarization, and dispersion/correlation energies all become increasingly attractive as the two subunits are forced closer together. The sole force that prevents such a collapse is the very rapid rise of the repulsion energy, highlighted in Figure S3c.

DISCUSSION

Given its electron-deficient character, Be usually behaves as a Lewis acid in the context of noncovalent interactions. But its coordination by three CO ligands with their extensive π-electron bonding, can lead to what is a sort of effective Be lone pair, capable of being donated to a Lewis acid unit. A noncovalent bond interpretation is further buttressed by the appearance of a negative MEP directly above the Be atom, a sort of π-lump, albeit not a strong one. One consequence of this weak π-lump is a correspondingly small electrostatic component of the triel bond energy with an assortment of TrX_3 units. In this same vein, the positive π-hole of TrX_3 is deepened as the X atom becomes more electronegative. However, this effect is mitigated by feedback bonding effects[22] whereby p_z orbitals of X transfer a certain amount of charge to the Tr center. This feedback is reduced for larger Tr atoms, and is absent for X = H which has no p-electrons. Another reason to think that electrostatics play a less major role in these interactions is the poor correlation between the TrB strength and the depth of the π-hole on TrX_3, which tends to stronger bonds with X atoms of lesser electronegativity for some of the complexes.

To confirm the reliability of the B3LYP-D3(BJ) method, two other DFT functionals, M06-2X and ωB97XD, were applied to calculate the interaction energy of each complex. Table S2 reports these results alongside the B3LYP-D3(BJ) data for ease of comparison. It is readily apparent that there are only small differences from one method to the next. Most importantly, the B3LYP-D3(BJ) values differ from the most accurate CCSD(T) by only 1 kcal/mol or less. The other two DFT functionals yield similar quantities, and preserve the same patterns as is seen with B3LYP-D3(BJ).

It is worth noting the variability of substituent effect with size of the central Tr atom. For the smaller B and Al atoms, E_{int} rises with size of X, while the opposite pattern characterizes the larger Tr atoms. Some of these patterns can be again connected with the aforementioned feedback bonding effects that diminish with larger Tr atoms. In the particular case of B, the same order was found in a previous Tr···N TrB study,[51] which found that the TrB between pyrazine and BX_3 varies in the order F > H > Cl > Br. On the other hand this same work found a different order for the Al TrBs, in that the Al···N TrB strength increases with the electronegativity of the X substituent.

The dominant component in the interaction energies of these dyads is the induction energy, much more sizable than electrostatic forces, making these TrBs a bit of an exception in the domain of noncovalent bonding. This component is in turn derived from an overlap of two particular molecular orbitals. The donor is the $Be(CO)_3$ HOMO, which has the outward appearance of a Be lone pair, but is in fact the coalescence of the π-bonding orbitals of the three CO ligands. The electron-accepting LUMO of the pyramidal TrX_3 resembles a vacant Tr lone pair orbital and is perfectly aligned with the $Be(CO)_3$ HOMO. The high degree of resulting charge transfer, as much as 1.0*e* in some cases, presents the interaction as containing a certain degree of dative bond character. The high covalent contribution is supported by the bond path between Be and Tr, with AIM quantities that border on covalency. The direct bonding along the Be···Tr axis is confirmed by IRI analysis, which also confirmed the involvement of the CO ligands, the latter of which found further verification via NOCV orbitals.

Ariyarathna and Miliordos found in a theoretical study of $Be(CX)_3$ (X = O, S, Se, Te, and Po), $Be(NH_3)_3$, and $Be(PH_3)_3$[33] that when the p_z orbitals of Be are filled with electrons, the electrons in this orbital shift toward the three ligands in the form of a feedback bond; in the case of $Be(CX)_3$, this lone electron pair Be p_z orbital conjugates with the three C−X π-bonds, forming delocalized π-bonds. This phenomenon was also pointed out by De and Parameswaran et al., who found that the lone electron pair in the Be $2p_z$ orbital is stabilized by π-feedback and hyperconjugation, and that the lone electron pair in the Be $2p_z$ orbital is usually hidden but highly reactive when interacting with electron-deficient molecules.[36] A very recent work[52] emphasized the manner in which $Be(CO)_n$ can be stabilized by donation from the CO bonding orbitals to the central Be, complemented by back-donation from the Be p_z orbital, consistent with our finding of charge transfer from the delocalized π-bonds in $Be(CO)_3$ to the Tr p_z orbital. With the exception of BF_3, the NOCV orbital interaction is the strongest in the B systems, in agreement with a study of Tr···N TrB.[53] It is finally pointed out that there is an analogy between the trigonal planar $Be(CO)_3$ unit and square-planar Pt(II) and Ir(I) systems[54] as partners with a series of TrX_3 molecules. In these cases, it is the doubly occupied d_{z^2}

https://doi.org/10.1021/acs.inorgchem.4c02186
Inorg. Chem. 2024, 63, 14656−14664

orbital of the metal that acts as the source of charge transfer to Tr.

CONCLUSIONS

The electronic structure of $Be(CO)_3$ provides first a negative π-lump in its MEP directly above the Be atom. Its orbital structure includes a HOMO in which three π(CO) bonding orbitals coalesce into what resembles a lone electron pair above the Be. This Be atom can thus engage directly as a Lewis base in a strong triel bond with the central triel atom of a TrX_3 molecule and its deep π-hole and vacant Tr p_z orbital. This TrB differs from many other noncovalent bonds in its dominating influence of polarization energy, and a surprisingly large total charge transfer from $Be(CO)_3$ to TrX_3. The interaction energy of this TrB is rather large, up to nearly 40 kcal/mol in some cases. In concert with the AIM characteristics of the Be···Tr bond critical point, these issues lead to the conclusion that this interaction borders on covalency. In a finer context, the dependence of the bond strength upon the nature of the substituents on the Tr atom varies according to the size of the central Tr.

ASSOCIATED CONTENT

Supporting Information

The Supporting Information is available free of charge at https://pubs.acs.org/doi/10.1021/acs.inorgchem.4c02186.

Tables (DOC) containing AIM data, method comparison, monomer distortions, local electron affinities, and figures (DOC) with IRI diagrams, distance dependence of various energy components, and Cartesian coordinates of minima (PDF)

AUTHOR INFORMATION

Corresponding Authors

Qingzhong Li − *The Laboratory of Theoretical and Computational Chemistry, School of Chemistry and Chemical Engineering, Yantai University, Yantai 264005, P. R. China;* orcid.org/0000-0003-1486-6772; Email: lqz@ytu.edu.cn

Steve Scheiner − *Department of Chemistry and Biochemistry, Utah State University, Logan, Utah 84322-0300, United States;* orcid.org/0000-0003-0793-0369; Email: steve.scheiner@usu.edu

Authors

Xin Wang − *The Laboratory of Theoretical and Computational Chemistry, School of Chemistry and Chemical Engineering, Yantai University, Yantai 264005, P. R. China*

Zhihao Niu − *The Laboratory of Theoretical and Computational Chemistry, School of Chemistry and Chemical Engineering, Yantai University, Yantai 264005, P. R. China*

Complete contact information is available at: https://pubs.acs.org/10.1021/acs.inorgchem.4c02186

Notes

The authors declare no competing financial interest.

ACKNOWLEDGMENTS

This work was supported by the Natural Science Foundation of Shandong Province (ZR2021MB123) and a grant to S.S. by the US National Science Foundation (1954310).

REFERENCES

(1) Zhang, W.; Nafady, A.; Shan, C.; Wojtas, L.; Chen, Y. S.; Cheng, Q.; Zhang, X. P.; Ma, S. Functional porphyrinic metal-organic framework as a new class of heterogeneous halogen-bond-donor catalyst. *Angew. Chem., Int. Ed.* **2021**, *60*, 24312.

(2) Xu, Y.; Hao, A.; Xing, P. X···X halogen bond-induced supramolecular helices. *Angew. Chem., Int. Ed.* **2022**, *61*, No. e202113786.

(3) Sutar, R. L.; Engelage, E.; Stoll, R.; Huber, S. M. Bidentate chiral bis (imidazolium)-based halogen-bond donors: Synthesis and applications in enantioselective recognition and catalysis. *Angew. Chem., Int. Ed.* **2020**, *59*, 6806−6810.

(4) Luo, Y.; Ma, H.; Zhang, S.; Zheng, D.; Che, P.; Liu, X.; Zhang, M.; Gao, J.; Xu, J. Binding energy as driving force for controllable reconstruction of hydrogen bonds with molecular scissors. *J. Am. Chem. Soc.* **2020**, *142*, 6085−6092.

(5) Bhunya, S.; Malakar, T.; Ganguly, G.; Paul, A. Combining protons and hydrides by homogeneous catalysis for controlling the release of hydrogen from ammonia-borane: Present status and challenges. *ACS Catal.* **2016**, *6*, 7907−7934.

(6) Hamilton, C. W.; Baker, R. T.; Staubitz, A.; Manners, I. B-N compounds for chemical hydrogen storage. *Chem. Soc. Rev.* **2009**, *38*, 279−293.

(7) Bismillah, A. N.; Aprahamian, I. Fundamental studies to emerging applications of pyrrole-BF_2(BOPHY)fluorophores. *Chem. Soc. Rev.* **2021**, *50*, 5631−5649.

(8) Grabowski, S. J. Boron and other triel Lewis acid centers: From hypovalency to hypervalency. *ChemPhysChem* **2014**, *15*, 2985−2993.

(9) Grotewold, J.; Lissi, E. A.; Villa, A. E. Reactions of co-ordinated boron compounds in the gas phase. Part I. Borine carbonyl and trimethylamine. *J. Chem. Soc. A* **1966**, 1034−1037.

(10) Herrebout, W. A.; Van der Veken, B. J. Van der Waals complexes between unsaturated hydrocarbons and boron trifluoride: An infrared and ab initio study of ethene●●●BF_3 and propene●●●BF_3. *J. Am. Chem. Soc.* **1997**, *119*, 10446.

(11) Fiacco, D. L.; Mo, Y.; Hunt, S. W.; Qtt, M. E.; Roberts, A.; Leopold, K. P. Dipole moments of partially bound Lewis acid-base adducts. *J. Phys. Chem. A* **2001**, *105*, 484−493.

(12) Reeve, S. W.; Burns, W. A.; Lovas, F. J.; Suenram, R. D.; Leopold, K. R. Microwave spectra and structure of hydrogen cyanide-boron trifluoride: An almost weakly bound complex. *J. Phys. Chem.* **1993**, *97*, 10630−10637.

(13) Phillips, J. A.; Giesen, D. J.; Wells, N. P.; Halfen, J. A.; Knutson, C. C.; Wrass, J. P. Condensed-phase effects on the structural properties of C_6H_5CN-BF_3 and $(CH_3)_3CCN$-BF_3: IR spectra, crystallography, and computations. *J. Phys. Chem. A* **2005**, *109*, 8199−8208.

(14) Leopold, K. R.; Canagaratna, M.; Phillips, J. A. Partially bonded molecules from the solid state to the stratosphere. *Acc. Chem. Res.* **1997**, *30*, 57−64.

(15) Pyykkö, P.; Atsumi, M. Molecular single-bond covalent radii for elements 1−118. *Chem.—Eur. J.* **2009**, *15*, 186−197.

(16) Hu, S. Z.; Zhou, Z. H.; Robertson, B. E. Consistent approaches to van der Waals radii for the metallic elements. *Z. Kristallogr.* **2009**, *224*, 375−383.

(17) Grabowski, S. J. π-Hole bonds: Boron and aluminum Lewis acid centers. *ChemPhysChem* **2015**, *16*, 1470−1479.

(18) Jonas, V.; Frenking, G.; Reetz, M. T. Comparative theoretical study of Lewis acid-base complexes of BH_3, BF_3, BCl_3, $AlCl_3$, and SO_2. *J. Am. Chem. Soc.* **1994**, *116*, 8741−8753.

(19) van der Veken, B. J.; Sluyts, E. J. Reversed Lewis acidity of mixed boron halides: An infrared study of the Van der Waals complexes of BF_xCl_y with CH_3F in cryosolution. *J. Am. Chem. Soc.* **1997**, *119*, 11516.

(20) Hiberty, P. C.; Ohanessian, G. Comparison of minimal and extended basis sets in terms of resonant formulas. Application to 1,3 dipoles. *J. Am. Chem. Soc.* **1982**, *104*, 66−70.

(21) Brinck, T.; Murray, J. S.; Politzer, P. A computational analysis of the bonding in boron trifluoride and boron trichloride and their complexes with ammonia. *Inorg. Chem.* **1993**, *32*, 2622−2625.
(22) Kutzelnigg, W. Chemical bonding in higher main group elements. *Angew. Chem., Int. Ed.* **1984**, *23*, 272−295.
(23) Rowsell, B. D.; Gillespie, R. J.; Heard, G. L. Ligand close-packing and the Lewis acidity of BF_3 and BCl_3. *Inorg. Chem.* **1999**, *38*, 4659−4662.
(24) Bessac, F.; Frenking, G. Why is BCl_3 a stronger Lewis acid with respect to strong bases than BF_3? *Inorg. Chem.* **2003**, *42*, 7990−7994.
(25) Phillips, J. A. Structural and energetic properties of nitrile-BX_3 complexes: Substituent effects and their impact on condensed-phase sensitivity. *Theor. Chem. Acc.* **2017**, *136*, 16.
(26) Giesen, D. J.; Phillips, J. A. Structure, bonding, and vibrational frequencies of CH_3CN-BF_3: New insight into medium effects and the discrepancy between the experimental and theoretical geometries. *J. Phys. Chem. A* **2003**, *107*, 4009−4018.
(27) Phillips, J. A.; Cramer, C. J. B-N distance potential of CH_3CN-BF_3 revisited: Resolving the experiment-theory structure discrepancy and modeling the effects of low-dielectric environments. *J. Phys. Chem. B* **2007**, *111*, 1408−1415.
(28) Wrass, J. P.; Sadowsky, D.; Bloomgren, K. M.; Cramer, C. J.; Phillips, J. A. Quantum chemical and matrix-IR characterization of CH_3CN-BCl_3: A complex with two distinct minima along the B-N bond potential. *Phys. Chem. Chem. Phys.* **2014**, *16*, 16480−16491.
(29) Grabowski, S. J. The nature of triel bonds, a case of B and Al centres bonded with electron rich sites. *Molecules* **2020**, *25*, 2703.
(30) Wang, X.; Li, B.; Li, Y.; Wang, H.; Ni, Y.; Wang, H. The influence of monomer deformation on triel and tetrel bonds between TrR_3/TR_4 (Tr = Al, Ga, In; T = Si, Ge, Sn) and N-base (N-base = HCN, NH_3, CN^-). *Comput. Theor. Chem.* **2021**, *1201*, 113268.
(31) Liu, G.; Fedik, N.; Martinez-Martinez, C.; Ciborowski, S. M.; Zhang, X.; Boldyrev, A. I.; Bowen, K. H Realization of Lewis basic sodium anion in the $NaBH_3^-$ cluster. *Angew. Chem., Int. Ed.* **2019**, *58*, 13789.
(32) Montero-Campillo, M. M.; Alkorta, I.; Elguero, J. Fostering the basic instinct of boron in boron-beryllium interactions. *J. Phys. Chem. A* **2018**, *122*, 3313−3319.
(33) Ariyarathna, I. R.; Miliordos, E. Dative bonds versus electron solvation in tri-coordinated beryllium complexes: $Be(CX)_3$ [X = O, S, Se, Te, Po] and $Be(PH_3)_3$ versus $Be(NH_3)_3$. *Int. J. Quantum Chem.* **2018**, *118*, No. e25673.
(34) Haynes, W. M.; Lide, D. R.; Bruno, T. J. *CRC Handbook of Chemistry and Physics*; CRC Press, 2016.
(35) Li, Y.; Mondal, K. C.; Lübben, J.; Zhu, H.; Dittrich, B.; Purushothaman, I.; Parameswaran, P.; Roesky, H. W. A functionalized Ge_3-compound with a dual character of the central germanium atom. *Chem. Commun.* **2014**, *50*, 2986−2989.
(36) De, S.; Parameswaran, P. Neutral tricoordinated beryllium(0) compounds- isostructural to BH_3 but isoelectronic to NH_3. *Dalton Trans.* **2013**, *42*, 4650−4656.
(37) Frisch, M. J.; Trucks, G. W.; Schlegel, H. B.; Scuseria, G. E.; Robb, M. A.; Cheeseman, J. R.; Scalmani, G.; Barone, V.; Mennucci, B.; Petersson, G. A.; Nakatsuji, H.; Caricato, M.; Li, X.; Hratchian, H. P.; Izmaylov, A. F.; Bloino, J.; Zheng, G.; Sonnenberg, J. L.; Hada, M.; Ehara, M.; Toyota, K.; Fukuda, R.; Hasegawa, J.; Ishida, M.; Nakajima, T.; Honda, Y.; Kitao, O.; Nakai, H.; Vreven, T.; Montgomery, J. J. A.; Peralta, J. E.; Ogliaro, F.; Bearpark, M.; Heyd, J. J.; Brothers, E.; Kudin, K. N.; Staroverov, V. N.; Kobayashi, R.; Normand, J.; Raghavachari, K.; Rendell, A.; Burant, J. C.; Iyengar, S. S.; Tomasi, J.; Cossi, M.; Rega, N.; Millam, J. M.; Klene, M.; Knox, J. E.; Cross, J. B.; Bakken, V.; Adamo, C.; Jaramillo, J.; Gomperts, R.; Stratmann, R. E.; Yazyev, O. A.; Austin, J.; Cammi, R.; Pomelli, C.; Ochterski, J. W.; Martin, R. L.; Morokuma, K.; Zakrzewski, V. G.; Voth, G. A.; Salvador, P.; Dannenberg, J. J.; Dapprich, S. A.; Daniels, D.; Farkas, O.; Foresman, J. B.; Ortiz, J. V.; Cioslowski, J.; Fox, D. J. *Gaussian 09*, Revision A.02, Gaussian Inc., Wallingford, CT, 2009.
(38) Becke, A. D. Density-functional thermochemistry. I. The effect of the exchange-only gradient correction. *J. Chem. Phys.* **1992**, *96*, 2155−2160.
(39) Peterson, K. A.; Shepler, B. C.; Figgen, D.; Stoll, H. On the spectroscopic and thermochemical properties of ClO, BrO, IO, and their anions. *J. Phys. Chem. A* **2006**, *110*, 13877−13883.
(40) Wilson, A. K.; Woon, D. E.; Peterson, K. A.; Dunning, T. H. Gaussian basis sets for use in correlated molecular calculations. IX. The atoms gallium through krypton. *J. Chem. Phys.* **1999**, *110*, 7667−7676.
(41) Boys, S. F.; Bernardi, F. The calculation of small molecular interactions by the differences of separate total energies. Some procedures with reduced errors. *Mol. Phys.* **1970**, *19*, 553−566.
(42) Lu, T.; Chen, F. W. Multiwfn: A multifunctional wavefunction analyzer. *J. Comput. Chem.* **2012**, *33*, 580−592.
(43) Bader, R. F. W. Atoms in molecules. *Acc. Chem. Res.* **1985**, *18*, 9−15.
(44) Lu, T.; Chen, Q. Interaction region indicator: A simple real space function clearly revealing both chemical bonds and weak interactions. *Chem.: Methods* **2021**, *1*, 231−239.
(45) Mitoraj, M. P.; Michalak, A.; Ziegler, T. A combined charge and energy decomposition scheme for bond analysis. *J. Chem. Theory Comput.* **2009**, *5*, 962−975.
(46) Tang, Z.; Song, Y. L.; Zhang, S.; Wang, W.; Xu, Y.; Wu, D.; Wu, W.; Su, P. F. XEDA, a fast and multipurpose energy decomposition analysis program. *J. Comput. Chem.* **2021**, *42*, 2341−2351.
(47) Su, P. F.; Tang, Z.; Wu, W. Generalized Kohn-Sham energy decomposition analysis and its applications. *Wiley Interdiscip. Rev. Comput. Mol. Sci.* **2020**, *10*, No. e1460.
(48) Zou, J. *MOKIT Program*, 2023.
(49) Grabowski, S. J. Triel bond and coordination of triel centres-Comparison with hydrogen bond interaction. *Coord. Chem. Rev.* **2020**, *407*, 213171.
(50) Cremer, D.; Kraka, E. Chemical bonds without bonding electron density—Does the difference electron-density analysis suffice for a description of the chemical bond? *Angew. Chem., Int. Ed.* **1984**, *23*, 627−628.
(51) Mariusz, M.; Zierkiewicz, W.; Scheiner, S. Triel-bonded complexes between TrR_3 (Tr = B, Al, Ga; R = H, F, Cl, Br, CH_3) and pyrazine. *ChemPhysChem* **2018**, *19*, 3122−3133.
(52) Purkayastha, S. K.; Rohman, S. S.; Parameswaran, P.; Guha, A. K. Beryllium carbonyl $Be(CO)_n$ (n = 1−4) complex: A p-orbital analogy of Dewar-Chatt-Duncanson model. *Phys. Chem. Chem. Phys.* **2024**, *26*, 12573.
(53) Li, Y.; Wang, X.; Wang, H. Influence of halogen atom substitution and neutral HCN/anion CN^- Lewis base on the triel-bonding interaction. *J. Mol. Model.* **2021**, *27*, 93.
(54) Chval, Z.; Dvořáčková, O.; Chvalová, D.; Burda, J. V. Square-planar Pt(II) and Ir(I) complexes as the Lewis bases: Donor-acceptor adducts with group 13 trihalides and trihydrides. *Inorg. Chem.* **2019**, *58*, 3616−3626.

https://doi.org/10.1021/acs.inorgchem.4c02186
Inorg. Chem. 2024, 63, 14656−14664